PNAS
www.pnas.org

Supplementary Information for

Engineered human antibodies for the opsonization and killing of *Staphylococcus aureus*

Xinhai Chen[1,2], Olaf Schneewind[†], Dominique Missiakas[1,2*]

Corresponding author: Dominique Missiakas
Email: dmissiak@bsd.uchicago.edu

This PDF file includes:

Figures S1 to S6
Tables S1 to S3

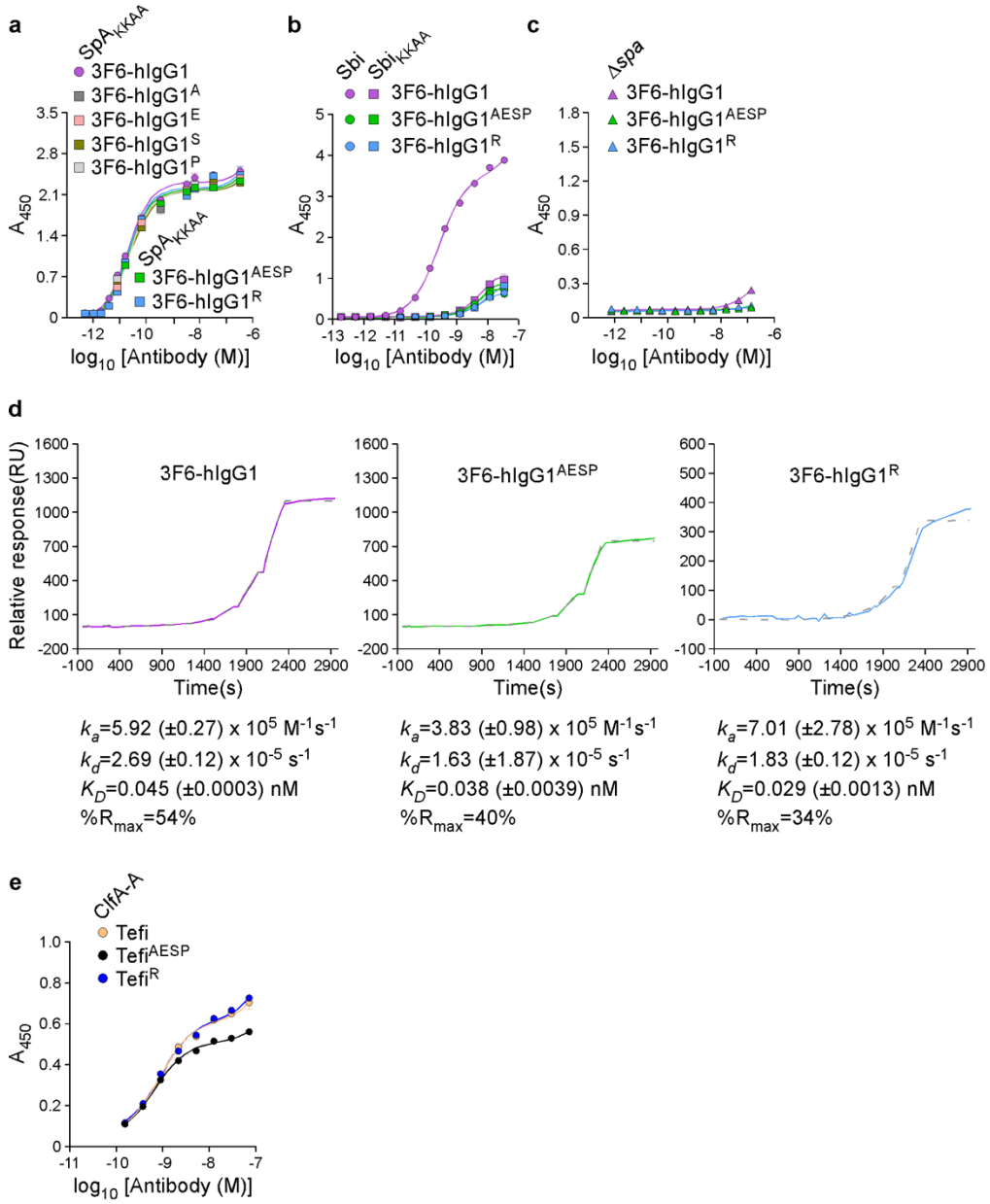

Fig. S1. Binding of staphylococcal antigens to cognate antibodies or their variants. Antibody interactions were measured by ELISA (**a-c, e**; n = 3 assays) and by surface plasmon resonance (SPR, Biacore 8K) (**d;** n = 2 assays). ELISA plates were coated with recombinant histidine tagged SpA$_{KKAA}$ (**a**), Sbi/Sbi$_{KKAA}$ proteins (**b**), Δ*spa* bacteria (**c**), recombinant histidine tagged ClfA-A domain (**e**). Bound antibodies were detected with HRP-conjugated secondary antibody and absorbances were recorded at 450 nm (A$_{450}$). **d**, SPR was used to determine the affinity of 3F6-hIgG1, 3F6-hIgG1^{AESP}, and 3F6-hIgG1^{R} to recombinant SpA$_{KKAA}$. Antigen (SpA$_{KKAA}$) was immobilized on NTA sensor chip. Eight concentrations (10, 3.3, 1.11, 0.37, 0.123, 0.041, 0.014, and 0.0046 nM) of each antibody were used to measure binding. Colored solid lines represent the acquired data and gray dotted lines which mostly overlap are fitting curves obtained with single-cycle

kinetics. Data are presented as mean ± s.e.m and are representative of two independent experiments.

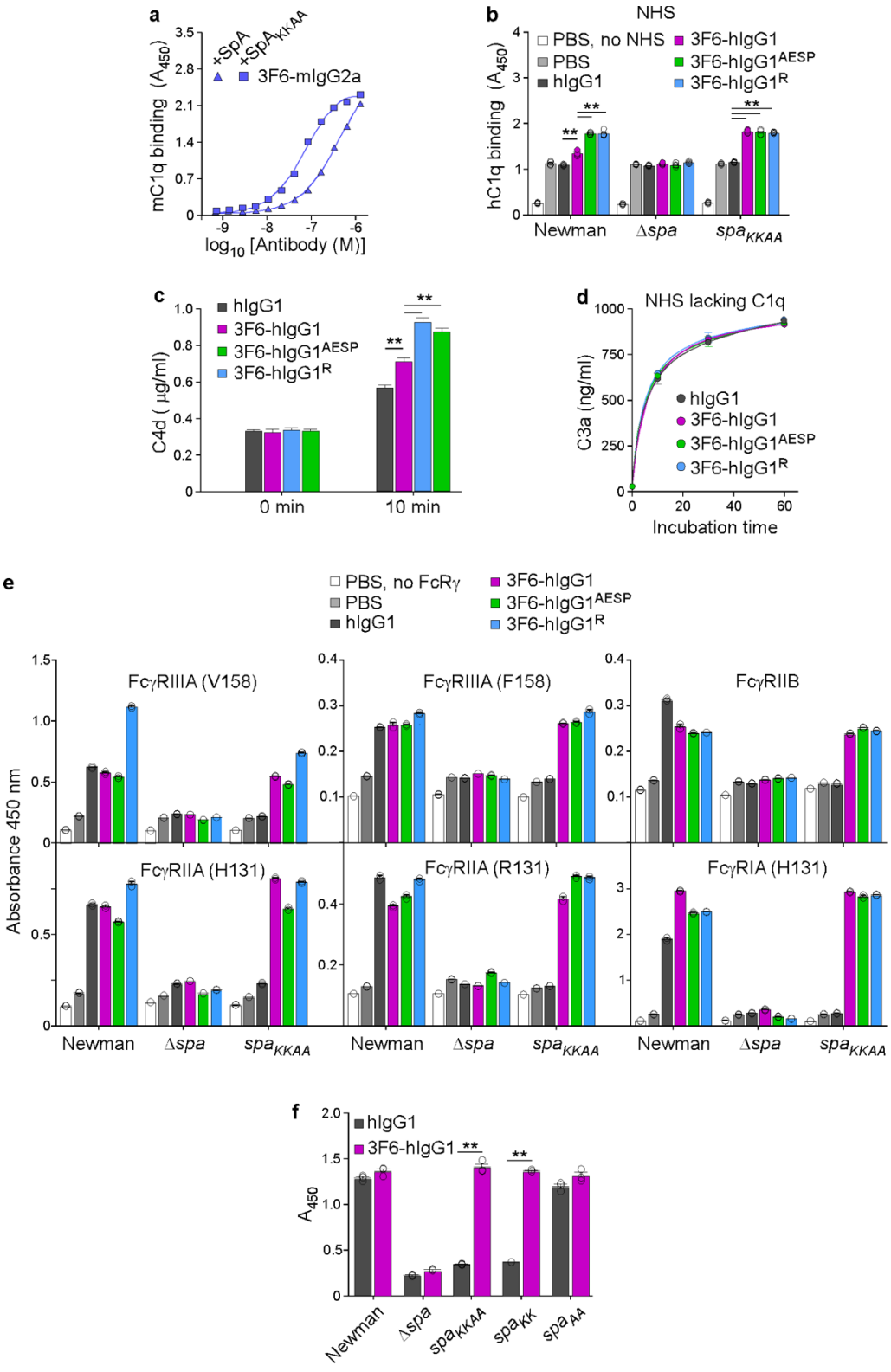

Fig. S2. SpA interaction with Fc blocks C1q but not FcγR binding. a, ELISA binding curves for (mouse) mC1q to 3F6-mIgG2a were assessed in the presence of SpA or

SpA_{KKAA} (n = 3 assays). **b**, hC1q binding to test antibody was assessed in the presence of bacteria: wild type Newman or its variants, Δ*spa* or spa_{KKAA}. ELISA plates were coated with bacteria. NHS was used as the source of hC1q. **c**, Quantification of C4d production following incubation with *S. aureus* Newman (1×10^8 CFU/ml) for 0 and 10 min in the presence of test antibodies and 10% NHS. **d**, Quantification of C3a production over time following incubation of bacteria (Newman 1×10^8 CFU/ml) with test antibodies and 10% NHS lacking hC1q. Data are presented as mean ± s.e.m (n = 3 assays). **e**, Binding of purified hFcγR to the surface of Newman or its variants, Δ*spa* or spa_{KKAA}, in the presence of test antibodies or PBS and hIgG1 controls (n = 3 assays). Color code for test antibodies is shown in the last panel. **f,** Antibody binding to Newman or its variants (Δ*spa*, spa_{KKAA}, spa_{KK}, or spa_{AA}) (n = 3 assays). Data are presented as mean ± s.e.m. Significant differences were identified in (**b**) by two-way ANOVA with Bonferroni post-tests (**$P < 0.01$; *$P < 0.05$) and in (**c**, **f**) by two-tailed Student's t-test (**$P < 0.01$; *$P < 0.05$). One representative of two independent experiments is shown.

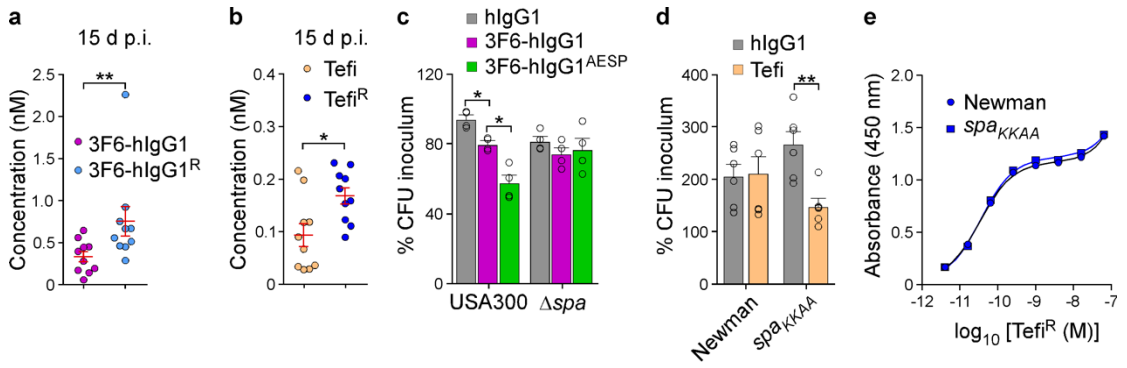

Fig. S3. Biological properties of anti-staphylococcal antibodies with Fc substitutions. **a-b,** Serum concentration of 3F6-hIgG1 and 3F6-hIgG1^{R} (**a**), and of Tefi and Tefi^{R} (**b**), in BALB/c mice 15 days post infection (p. i.). Animals were the same as in Fig. 2a-d. **c-e,** OPK activityof test antibodies toward *S. aureus* USA300 or its Δ*spa* variants ($n = 4$ donors) (**c**) and toward Newman and its *spa*$_{KKAA}$ variant ($n = 6$ donors) in human blood (**d**). **e,** Tefi^{R} binding to Newman or *spa*$_{KKAA}$ bacteria ($n = 3$ assays). ELISA plates were coated with bacteria. Data are presented as mean ± s.e.m. and differences identified with the two-tailed Student's *t* test (**a-b**) or two-way ANOVA with Bonferroni post-tests (**c-d**) (**$P < 0.01$; *$P < 0.05$).

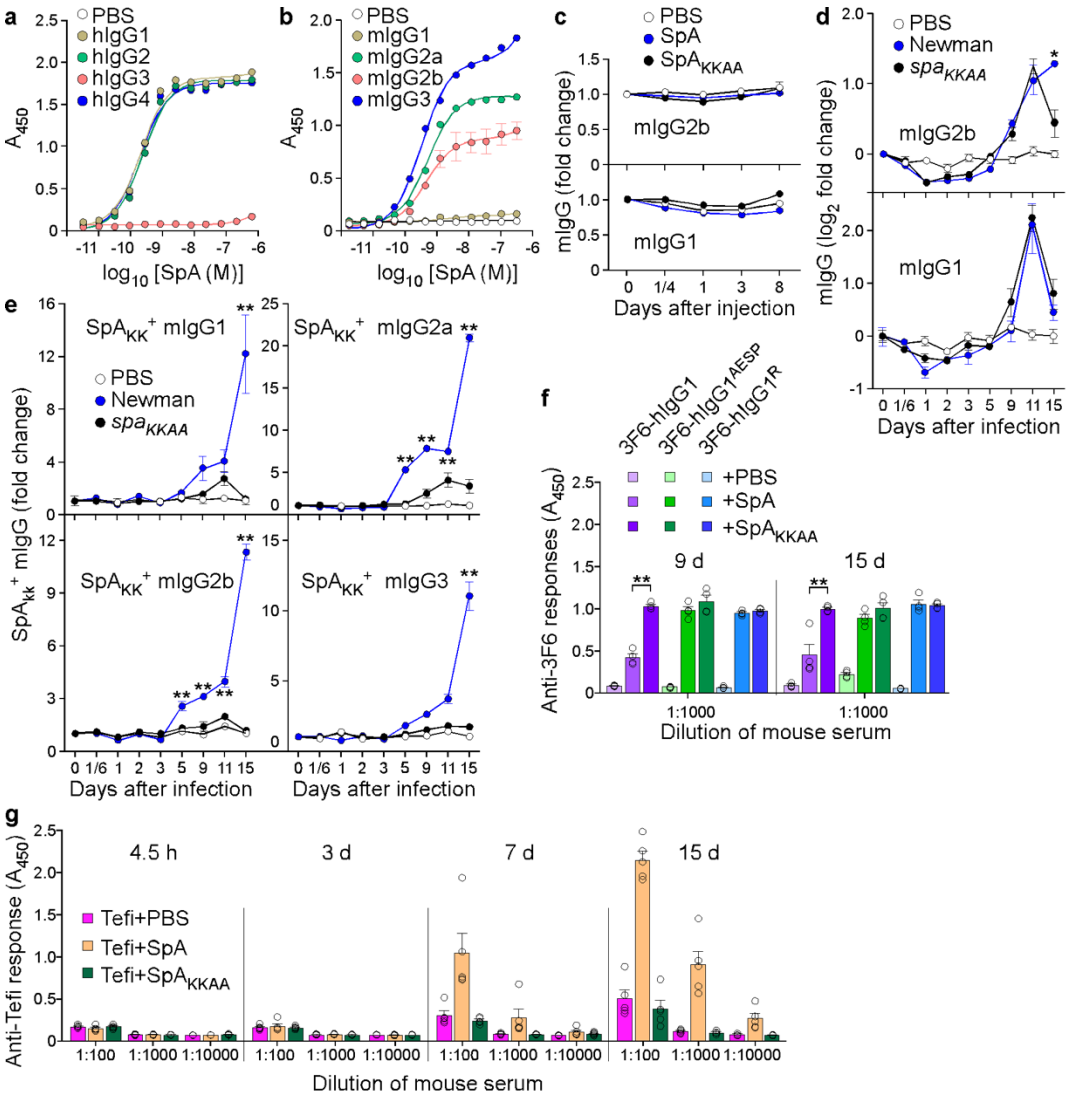

Fig. S4. Impact of SpA interactions with antibodies and immune complexes. a-b, ELISA binding curves for the indicated human (**a**) and mouse (**b**) IgG to SpA ($n = 3$ assays). ELISA plates were coated with IgG or mock (PBS). **c-d,** Fold change over time of the serum concentration of mIgG1 and mIgG2b following injection of PBS, SpA or SpA_{KKAA} (**c**), and of PBS, Newman or its *spa*$_{KKAA}$ variant in BALB/c mice (**d**) ($n = 4$ animals per group). **e**, Fold change over time of the serum concentration of V_H3-clonal mIgG from mice infected with mock (PBS), Newman or its *spa*$_{KKAA}$ variant. Sera were from animals shown in panel d and Fig. 4d. **f**, Antibody responses against antibodies 3F6-hIgG1, 3F6-hIgG1^R, and 3F6-hIgG1^{AESP} following injection in BALB/c mice ($n = 4$ animals per group) in the presence of SpA, SpA_{KKAA}, or PBS control. Sera were obtained from animals shown in Fig. 4f on days 9 and 15. **g**, Antibody responses against Tefi following injection in BALB/c mice ($n = 4$ animals per group) in the presence of SpA, SpA_{KKAA}, or PBS control. Sera were obtained from animals shown in Fig. 4g at the indicated times. Significant differences were identified in (**d**, **e**) by two-way ANOVA with Bonferroni post-tests and in **f** by one-way ANOVA with Tukey's multiple-comparison test (**$P < 0.01$; *$P < 0.05$).

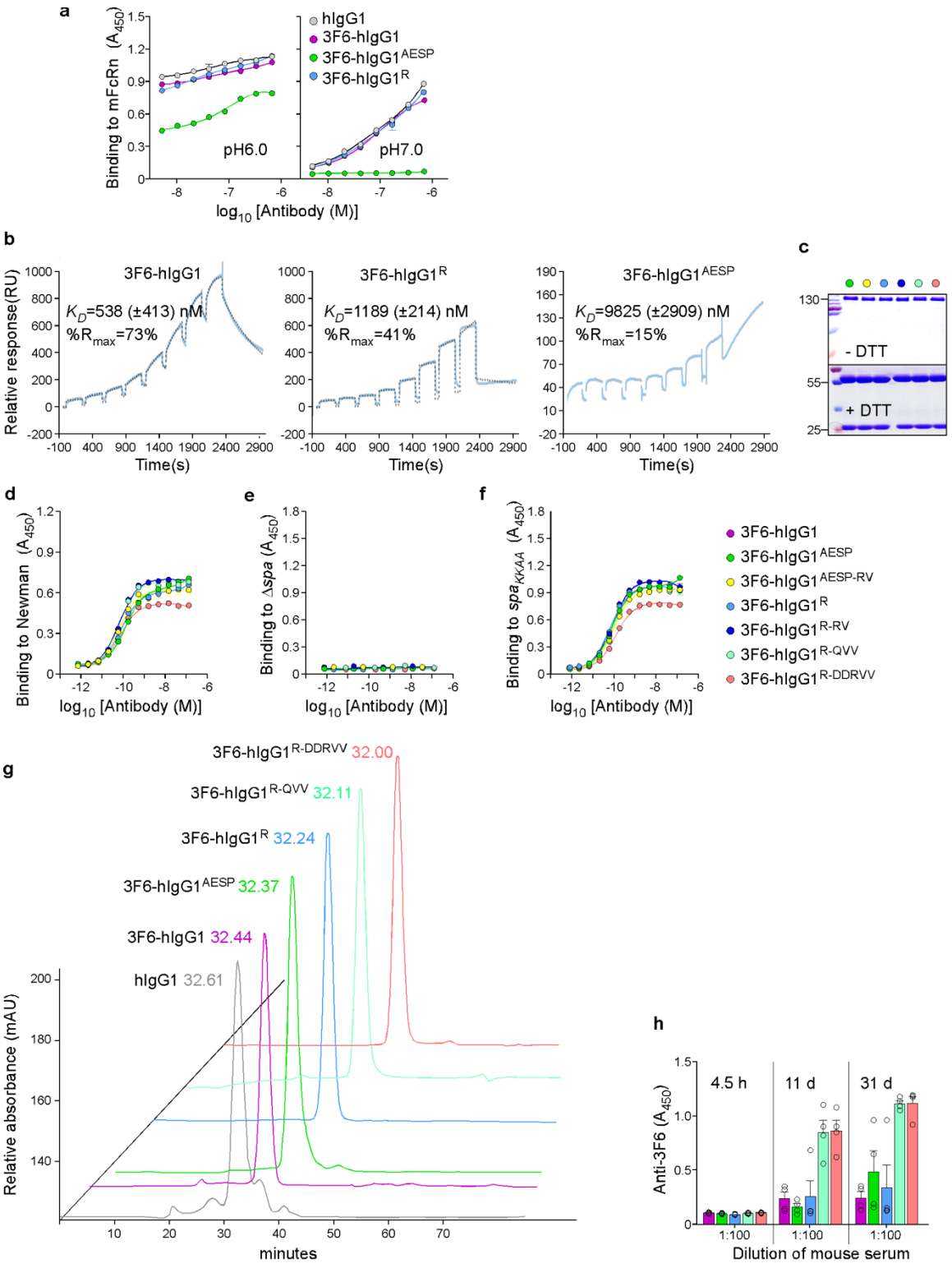

Fig. S5. Effect of 3F6 amino acid substitutions on FcRn and antigen binding and on immunogenicity. **a,** ELISA binding curves for mFcRn to antibodies were obtained at pH6.0 and pH7.0 (n = 3 assays). ELISA plates were coated with serially diluted test

antibodies. **b**, SPR binding curves of 3F6-hIgG1, 3F6-hIgG1^{AESP}, and 3F6-hIgG1^{R} at pH 6.0 to human FcRn (hFcRn) immobilized on NTA sensor chip. Eight concentrations (2500, 1250, 625, 312.5, 156.3, 78.1, 39.1, and 19.5 nM) of each antibody were used. Light blue lines represent experimental binding curves and gray dotted lines are calculated fit using single-cycle kinetics. **c**, Coomassie-stained gel following SDS-PAGE separation of 3F6-hIgG1 variants in the absence (-) or presence (+) of the reducing agent dithiothreitol (DTT). **d-f**, ELISA binding curves (n = 3 assays) for antibody variants to Newman (**d**), Δ*spa* (**e**), and *spa*$_{KKAA}$ (**f**) bacteria. ELISA plates were coated with bacteria. **g**, Size exclusion chromatography of purified hIgG1, 3F6-hIgG1, and 3F6-hIgG1 variants. **h**, Antibody responses against test antibodies following injection in BALB/c mice (n = 4 animals per group). Sera were obtained at indicated times from animals shown in Fig. 5e. Data are presented as mean ± s.e.m and representative of two independent experiments (**c**-**e**).

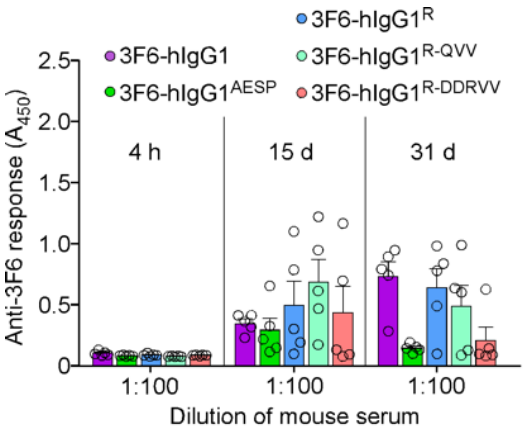

Fig. S6. Antibody responses against test antibodies following injection in Tg32 mice. Sera were obtained at indicated times from animals shown in Fig. 6c. Data are presented as mean ± s.e.m. No statistical difference could be found between the data.

Table S1. Half maximal effective concentration (EC_{50}) values for all binding experiments using ELISA

		Test antibodies									
Ligand	**EC_{50} (M)**	**3F6-hIgG1**	**3F6-hIgG1^{AESP}**	**3F6-hIgG1^{R}**	**SpA**	**SpA$_{KKAA}$**	**Tefi**	**Tefi^{AESP}**	**Tefi^{R}**	**3F6-hIgG1^{R-QVV}**	**3F6-hIgG1$^{R-DDRVV}$**
SpA	10^{-11}	36.16 ± 2.22	4.77 ± 0.49	4.90 ± 0.49	--	--	26.2 ± 1.77	<	<	--	--
SpA$_{KKAA}$	10^{-11}	8.80 ± 0.59	5.05 ± 0.34	4.82 ± 0.39	--	--	--	--	--	--	--
Newman	10^{-10}	5.58 ± 0.64	1.67 ± 0.17	1.81 ± 0.19	--	--	--	--	0.35 ± 0.027	0.69 ± 0.091	0.75 ± 0.097
Δ*spa*	10^{-10}	<	<	<	--	--	--	--	--	<	<
spa$_{KKAA}$	10^{-10}	1.01 ± 0.03	1.08 ± 0.05	1.07 ± 0.06	--	--	--	--	0.36 ± 0.032	0.99 ± 0.12	1.22 ± 0.13
3F6-hIgG1	10^{-11}	--	--	--	49.7 ± 6.67	10.1 ± 1.16	--	--	--	--	--
3F6-hIgG1^{AESP}	10^{-11}	--	--	--	35.5 ± 4.80	11.1 ± 1.08	--	--	--	--	--
3F6-hIgG1^{R}	10^{-11}	--	--	--	31.1 ± 4.42	10.8 ± 1.24	--	--	--	--	--
Sbi	10^{-10}	2.72 ± 0.14	<	<	--	--	1.08 ± 0.07	--	<	--	--
Sbi$_{KKAA}$	10^{-10}	<	<	<	--	--	<	--	<	--	--
ClfA-A	10^{-10}	--	--	--	--	--	2.61 ± 0.31	1.93 ± 0.23	2.83 ± 0.35	--	--
hc1q	10^{-7}	2.50 ± 0.42	1.23 ± 0.16	1.11 ± 0.11	--	--	0.38 ± 0.027	0.80 ± 0.041	0.56 ± 0.072	--	--
hFcRn pH6.0	10^{-8}	27.3 ± 1.07	<	<	--	--	0.63 ± 0.033	4.18 ± 0.56	0.67 ± 0.033	>	>
hFcRn pH7.0	10^{-8}	<	<	<	--	--	--	--	--	<	<
mFcRn pH6.0	10^{-8}	>	>	>	--	--	--	--	--	>	>
mFcRn pH7.0	10^{-8}	9.44 ± 1.93	<	4.78 ± 2.13	--	--	--	--	--	>	>

		Control antibodies							
Ligand	**EC50 (M)**	**hIgG1**	**hIgG2**	**hIgG3**	**hIgG4**	**mIgG1**	**mIgG2a**	**mIgG2b**	**mIgG3**
SpA	10^{-11}	19.9 ± 2.30	23.9 ± 2.29	<	19.6 ± 2.05	<	49.5 ± 4.93	49.7 ± 5.44	33.2 ± 3.27
hFcRn pH6.0	10^{-8}	8.74 ± 1.15	1.30 ± 0.06	--	1.27 ± 0.11	--	--	--	--
hFcRn pH7.0	10^{-8}	--	--	--	--	--	--	--	--
mFcRn pH6.0	10^{-8}	--	--	--	--	--	3.38 ± 0.13	4.06 ± 0.68	3.80 ± 0.23
mFcRn pH7.0	10^{-8}	--	--	--	--	--	--	--	--

Symbols were as follows: -- binding was not measured; < binding was too low to determine EC_{50} value; > binding was too high to determine EC_{50} value.

Table S2. EC_{50} between test antibodies and ligands (C1q/FcRn) in the presence of SpA competitor

		Competitor	
Binding pair	**EC_{50} (M)**	**SpA**	**SpA_{KKAA}**
3F6 hIgG1 & hc1q	10^{-7}	29.2 ± 45.1	1.27 ± 0.081
3F6-hIgG1^{AESP} & hc1q	10^{-7}	0.20 ± 0.022	0.30 ± 0.35
3F6-hIgG1^{R} & hc1q	10^{-7}	0.18 ± 0.022	0.27 ± 0.029
3F6-hIgG1$^{R\text{-}QVV}$ & hc1q	10^{-7}	0.27 ± 0.036	0.29 ± 0.036
3F6-hIgG1$^{R\text{-}DDRVV}$ & hc1q	10^{-7}	0.57 ± 0.010	0.65 ± 0.015
Tefi & hc1q	10^{-7}	1.21 ± 0.14	0.39 ± 0.018
Tefi^{AESP} & hc1q	10^{-7}	0.75 ± 0.048	0.84 ± 0.053
Tefi^{R} & hc1q	10^{-7}	0.47 ± 0.050	0.46 ± 0.055
3F6-mIgG2a & mc1q	10^{-7}	4.22 ± 0.72	0.82 ± 0.096
hIgG1 & hFcRn pH6.0	10^{-8}	<	5.94 ± 1.03
hIgG2 & hFcRn pH6.0	10^{-8}	<	1.57 ± 0.17
hIgG4 & hFcRn pH6.0	10^{-8}	<	1.08 ± 0.18
Tefi & hFcRn pH6.0	10^{-8}	4.98 ± 0.21	0.63 ± 0.039
mIgG2a & mFcRn pH6.0	10^{-8}	<	<
mIgG2b & mFcRn pH6.0	10^{-8}	<	<
mIgG3 & mFcRn pH6.0	10^{-8}	<	<

The symbol "<" indicates that interactions between antigen and ligand (binding pairs) were inhibited even at the lowest concentration of competitor.

Table S3. Non-compartmental pharmacokinetic (PK) parameters for test antibodies in mice.

	BALB/c mice - PK parameters[1]			
Antibody	**$t_{1/2}$ (d)**	**C_{max} (nM)**	**$AUC_{0\text{-}inf}$ (nM*d)**	**Clearance ((mg/kg)/nM/d)**
3F6-hIgG1	10.1	923.9	12848.5	0.00039
3F6-hIgG1^{R}	8.3	1152.4	23156.3	0.00022
3F6-hIgG1^{AESP}	8.6	786.8	10775.8	0.00046
3F6-hIgG1$^{R\text{-}QVV}$	3.1	710.8	3753.6	0.00133
3F6-hIgG1$^{R\text{-}DDRVV}$	2.3	948.8	5004.45	0.00099
	Tg32 mice - PK parameters			
Antibody	**$t_{1/2}$ (d)**	**C_{max} (nM)**	**$AUC_{0\text{-}inf}$ (nM*d)**	**Clearance ((mg/kg)/nM/d)**
3F6-hIgG1	8.7	693.5	6737.8	0.00074
3F6-hIgG1^{R}	10.0	535.2	7235.9	0.00069
3F6-hIgG1^{AESP}	1.4	641.7	1171.9	0.00427
3F6-hIgG1$^{R\text{-}QVV}$	10.5	525.2	8401.8	0.00060
3F6-hIgG1$^{R\text{-}DDRVV}$	7.9	575.4	5964.5	0.00084
	Tg32 pretreated with hIgG - PK parameters			
Antibody	**$t_{1/2}$ (d)**	**C_{max} (nM)**	**$AUC_{0\text{-}inf}$ (nM*d)**	**Clearance ((mg/kg)/nM/d)**
3F6-hIgG1	12.0	302.8	6524.6	0.00077
3F6-hIgG1^{R}	15.2	278.2	7765.4	0.00064
3F6-hIgG1^{AESP}	not determined	not determined	not determined	not determined
3F6-hIgG1$^{R\text{-}QVV}$	20.0	323.4	12319.6	0.00041
3F6-hIgG1$^{R\text{-}DDRVV}$	14.6	340.3	7266.8	0.00069

[1]PK parameters: $t_{1/2}$, terminal half-life; C_{max}, Maximum concentration; AUC: Area under the concentration-time curve (AUC); Clearance: Systemic clearance.